Room-temperature lasing action in $In_{0.51}Ga_{0.49}P/In_{0.2}Ga_{0.8}As$ microcylinder laser diodes

A. F. J. Levi, R. E. Slusher, S. L. McCall, S. J. Pearton, and W. S. Hobson
AT&T Bell Laboratories, Murray Hill, New Jersey 07974

(Received 17 September 1992; accepted for publication 2 February 1993)

We report room-temperature operation of electrically pumped whispering-gallery mode $In_{0.51}Ga_{0.49}P/In_{0.2}Ga_{0.8}As$ microcylinder laser diodes with emission at wavelength $\lambda=1.0$ μm and threshold current $I_{th}=5$ mA. Because the lasing modes do not overlap the diode's central region, carrier density is not efficiently pinned by above-threshold stimulated emission.

Recently we demonstrated use of whispering-gallery modes at the edge of a semiconductor disk as the resonant cavity of a laser. We showed lasing action at a wavelength $\lambda=1.5$ μm in optically pumped $In_{0.53}Ga_{0.47}As$ microdisks at liquid nitrogen temperatures[1] and in electrically pumped p-n diode structures at room temperature.[2] Lasing in microdisks less than 10 μm in diameter is possible through use of high Q of whispering-gallery modes. Of course, a consequence of using very high Q resonators is that not much lasing light radiates out into free space. In Ref. 3 we demonstrated that the use of light output couplers, which slightly spoil Q, allow the output light to be efficiently increased and redirected. There are, however, other issues which must be addressed if microlasers are to find practical application.

We extend whispering-mode laser geometry from microdisks to microcylinders and report lasing action at a wavelength $\lambda=1.0$ μm. This study reveals the important role spontaneous emission plays in determining the performance of both microdisk and microcylinder lasers. We find that the presence of carriers that are weakly coupled to the lasing mode results in a reduction in laser efficiency. Estimates derived from rate equation modeling suggest a factor 1.5 reduction in efficiency due to this effect.

The devices used in this study were fabricated from epitaxial layers of InGaAsP grown by metalorganic chemical vapor deposition (MOCVD) on a GaAs substrate at 625 °C. The n-type substrate normal is oriented 2° off the ⟨100⟩ towards the ⟨110⟩ direction. The layer structure used is depicted in Table I. First, an n-type GaAs buffer layer is grown. This is followed by a 1.2 μm thick layer of $In_{0.51}Ga_{0.49}P$ Si-doped to $n=1.5\times10^{18}$ cm^{-3}. The gain region of the structure consists of three 80 Å thick $In_{0.2}Ga_{0.8}As$ strained quantum wells separated by 100 Å thick GaAs barriers. The quantum wells are sandwiched between two 1200 Å thick GaAs layers. The structure is completed by growing a 1.2 μm thick layer of $In_{0.51}Ga_{0.49}P$ Zn-doped to $p=1\times10^{18}$ cm^{-3} followed by thin heavily p-type GaAs and InGaAs contact layers.

After removal from the growth chamber microcylinder lasers are fabricated using photolithographic and dry-etching techniques. Figure 1(a) shows a scanning electron microscope (SEM) image of a 6 μm diameter 3.5 μm high microcylinder. The AuBe/Au alloyed metal contact to the p-type $In_{0.2}Ga_{0.8}As$ contact layer is visible. In Fig. 1(b) we show a SEM image of a completed structure with polyimide planarization and a Ti/Au metal line making electrical connection to the AuBe/Au metallization. A NiGeAu alloy is used for ohmic contact to the n-type GaAs substrate.

In Fig. 2 we show typical room-temperature pulsed current-light characteristics for a 9 μm diam microcylinder laser diode. Electrical pulses are 0.1 μs long with a 1000:1 duty cycle. Light intensity L emitted in the plane, is collected using a lensed multimode fiber placed 100 μm from the device. We estimate that the fiber collects at most a few percent of the emitted radiation. Lasing threshold ($I_{th}=5$ mA) causes a kink in the L-I characteristic. The relatively small contribution of lasing light above threshold and the high level of collected incoherent light below threshold is typical of these devices. Similar behavior, as mentioned in Ref. 2 is observed in $In_{0.53}Ga_{0.47}As/InP$ microdisk emitting at $\lambda=1.5$ μm which have room-temperature threshold currents around $I_{th}=1$ mA.

In Figs. 3(a) and 3(b) we show spectra from the device used for Fig. 2 with currents $I=14$ mA and $I=50$ mA, respectively. The spectrometer resolution is 50 Å. It is clear from Fig. 3(a) that there is a significant contribution to total light intensity at wavelengths other than the lasing line at $\lambda=1.034$ μm. Figure 3(b) shows that at high pumping levels lasing into several modes occurs. The measured mode spacing of $\Delta\lambda=90$ Å is consistent with that expected for whispering-gallery modes ($\Delta\lambda=\lambda^2/\pi\, dn_g$ where $d=9$ μm is the diameter of the cylinder and $n_g=4$ is the semiconductor's refractive index). In addition, inspection of Fig. 3 reveals that there is a substantial increase of

TABLE I. Layer structure.

Material	Thickness (μm)	Impurity concentration (cm^{-3})
$In_{0.2}Ga_{0.8}As$	0.01	$p=2.0\times10^{19}$
GaAs	0.29	$p=2.0\times10^{19}$
$In_{0.5}Ga_{0.5}P$	1.2	$p=1.0\times10^{18}$
GaAs	0.12	i
$In_{0.2}Ga_{0.8}As$	0.008	i
GaAs	0.01	i
$In_{0.2}Ga_{0.8}As$	0.008	i
GaAs	0.01	i
$In_{0.2}Ga_{0.8}As$	0.008	i
GaAs	0.12	i
$In_{0.5}Ga_{0.5}P$	1.2	$n=1.5\times10^{18}$
GaAs	0.5	$n=2.0\times10^{18}$
GaAs	substrate	$n=3.0\times10^{18}$

 0003-6951/93/172021-03$06.00

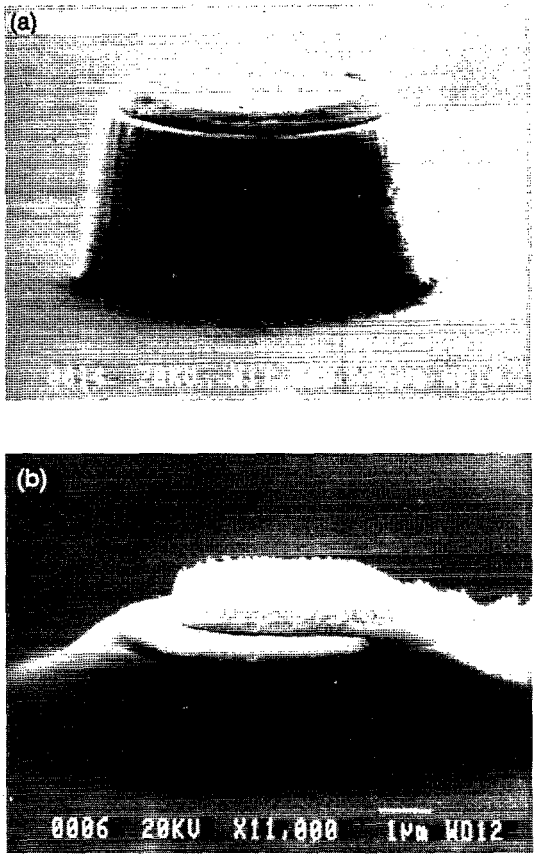

FIG. 1. (a) SEM image of partially completed microcylinder laser diode structure. The cylinder is 6 μm in diameter and 3.5 μm high. (b) SEM view of completed device with polyimide planarization.

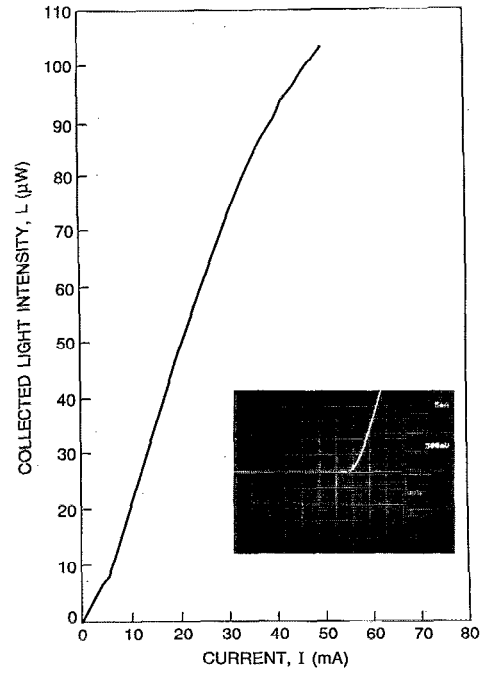

FIG. 2. Measured collected light output L as a function of current I. Threshold current is $I_{th}=5$ mA. Measurements were performed at room temperature ($T=300$ K) using 0.1 μs current pulses with a 1000:1 duty cycle. Inset shows the current-voltage characteristic of the laser diode. The diode has a series resistance of $R_s<30\ \Omega$.

incoherent spontaneous emission background with increasing current above threshold. This demonstrates that stimulated emission in the various lasing modes fail to pin (see p. 55 of Ref. 4) carrier density everywhere in this device.

Such ineffective carrier pinning is a consequence of the fact that optical field intensity of low loss whispering-gallery modes is small away from the edge of the cylinder. There is essentially no modal intensity overlap with carriers near the center of the cylinder. Hence, on length scales greater than the electron and hole diffusion length, carriers in this central region are not effectively pinned by lasing in whispering-gallery modes. At high carrier concentrations of $n=10^{19}$ cm^{-3} electron and hole diffusion lengths are approximately 1 μm at room temperature. We note that spontaneous and amplified spontaneous emission into other modes contributes to diffusion of carriers via reabsorption at the cylinder's edge. This is especially important for modes with small radial quantum number whose spatial location is near that of lasing modes. Obviously, accurately modeling such behavior is somewhat complicated and beyond the scope of commonly used single-mode rate equations (see, for example, Ref. 4). A naive approach involves modification of the rate equations to explicitly take into account the lack of carrier pinning gain compression ε and allowance of a carrier density dependent spon-

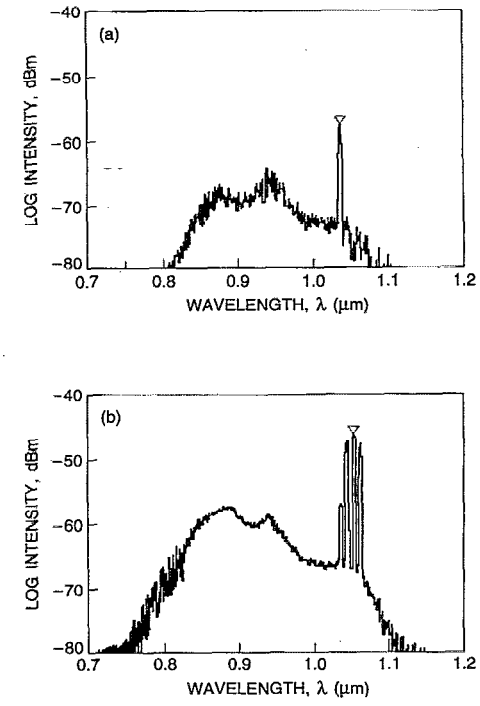

FIG. 3. (a) Measured room-temperature spectrum for injection current of $I=14$ mA. The triangle marks the peak in single mode lasing emission at $\lambda=1.034$ μm. (b) Measured room-temperature spectrum for injection current of $I=50$ mA. The triangle marks the emission peak for $\lambda=1.049$ μm. At these high drive currents the emission spectrum is multimode.

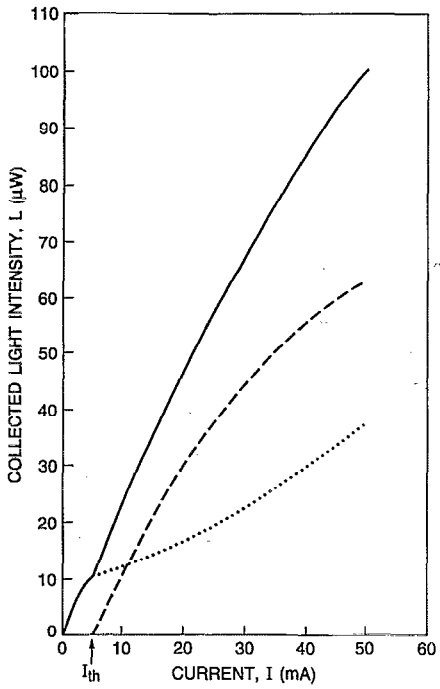

FIG. 4. Results of a rate equation model to calculate *L-I* characteristics of a device similar to that used for Figs. 2 and 3. Total collected light intensity L is shown as the solid curve. The broken curve is the calculated intensity of the lasing line. The dotted curve is the contribution from spontaneous emission. Threshold current is $I_{th}=5$ mA.

taneous emission factor, β. Here, β is the fraction of spontaneous emission rate into the lasing mode. In our model we simply set $\beta(n)=\beta_0(n_0/n)$ for $n>n_0$ and $\beta=\beta_0$ for $n<n_0$, where $\beta_0=2\times10^{-5}$ and $n_0=1\times10^{18}$ cm^{-3} is carrier density at transparency for the lasing mode. The rate equation for the photon intensity, S, is $dS/dt=(g-\kappa)S+\beta r_{sp}$ where gain $g=\beta\Gamma a(n-n_0)(1-\varepsilon S)$, a is a constant, Γ is the confinement factor, and κ is the optical loss rate. The carrier density evolves according to $dn/dt=I/ev-n/\tau_n-gS$, where v is the active volume and e the electron charge. The carrier recombination rate is $1/\tau_n=A+Bn+Cn^2$, and the spontaneous emission rate is $r_{sp}=Bn^2$.

In Fig. 4 we show results of calculating the measured *L-I* characteristics using such a modified rate equation model in which carrier density in the center of the cylinder is not effectively pinned by stimulated emission at the edge of the cylinder. In this model we take into account the fact that the fiber acts as an aperture which collects a fraction α_1 of spontaneously emitted and α_2 of lasing light. It is evident from Figs. 2 and 4 that the measured total light intensity ($L=\alpha_1 r_{sp}+\alpha_2 S$) agrees well with the results of the model. The broken curve in Fig. 4 is the calculated intensity of the lasing line with a threshold current around $I_{th}=5$ mA. The dotted curve is the contribution from spontaneous emission to the above threshold collected light level. The fact that spontaneous emission increases above threshold is a measure of the inability of stimulated emission to pin carrier density.

It is possible to circumvent ineffective carrier pinning by either reducing the radius of the microcylinder or changing the geometry of the device such that the optical mode effectively fills the entire gain region. An example of the latter is removal of the central section of the gain region. A reduction of cylinder radius can result in competing effects. For example, the lasing mode in a device with radius less than the carrier diffusion length should pin carrier density more effectively. On the other hand, for small resonators, the spontaneous emission factor is changed[5,6] resulting in less carrier pinning. This, combined with the fact that β depends on carrier density, can become an important factor determining device behavior.

In summary, for the first time we demonstrate room-temperature lasing action at wavelength $\lambda=1.0$ μm in electrically pumped whispering-gallery mode $In_{0.51}Ga_{0.49}P/In_{0.2}Ga_{0.8}As$ microcylinders. Spontaneous emission in the nonmodal region reduces the effect of carrier pinning above threshold. However, reduction of microcylinder or microdisk radius should result in improved device performance.

We thank R. A. Keane for providing SEM images.

[1] S. L. McCall, A. F. J. Levi, R. E. Slusher, S. J. Pearton, and R. A. Logan, Appl. Phys. Lett. **60**, 289 (1992).
[2] A. F. J. Levi, R. E. Slusher, S. L. McCall, T. Tanbun-Ek, D. L. Coblentz, and S. J. Pearton, Electron. Lett. **28**, 1010 (1992).
[3] A. F. J. Levi, R. E. Slusher, S. L. McCall, J. L. Glass, S. J. Pearton, and R. A. Logan, Appl. Phys. Lett. **62**, 561 (1993).
[4] G. P. Agrawal and N. K. Dutta, *Long-Wavelength Semiconductor Lasers* (Van Nostrand-Reinhold, New York, 1986).
[5] Y. Yamamoto, S. Machida, and G. Björk, Opt. Quantum Electron. **24**, S215 (1992).
[6] T. Baba, T. Hammano, F. Koyama, and K. Iga, IEEE J. Quantum Electron. **27**, 1347 (1992).